Pergamon

0277–5387(94)00430–7

Polyhedron Vol. 14, No. 12, pp. 1621–1639, 1995

0277–5387/95 $9.50+0.00

EPIMERIZATION OF CYANOCOBALAMIN. IMPROVED SYNTHESIS OF CYANO-8-EPICOBALAMIN AND ITS CHARACTERIZATION BY X-RAY CRYSTALLOGRAPHY, AND ^{1}H, ^{13}C, AND ^{15}N NMR

K. L. BROWN,* X. ZOU and G.-Z. WU

Department of Chemistry, Box CH, Mississippi State University, Mississippi State, MS 39762, U.S.A.

and

J. D. ZUBKOWSKI

Chemistry Department, Jackson State University, Jackson, MS 39217, U.S.A.

and

E. J. VALENTE

Department of Chemistry, Box 4065, Mississippi College, Clinton, MS 39085, U.S.A.

(*Received* 8 *August* 1994; *accepted* 14 *October* 1994)

Abstract—The structure of cyano-8-epicobalamin (CN-8-epiCbl), the C8 epimer of vitamin B_{12} (cyanocobalamin, CNCbl) has been determined by X-ray crystallography, complete assignment of its ^{1}H and ^{13}C NMR spectra, as well as observation and assignment of its amide ^{1}H and ^{15}N NMR spectra in DMSO-d_6. This compound was previously reported as the poorly characterized product of the amidation of its *c*-monocarboxylate, obtained as a minor product of the borohydride reduction of cobalamin-*c*-lactone. The conditions for the key epimerization step have now been changed to provide a tripling of the yield of the 8-epi-*c*-monocarboxylate. Along with substantial improvement in the procedures for synthesizing cobalamin-*c*-lactone and for amidating the monocarboxylate, this modified method for epimerization of cyanocobalamin now provides CN-8-epiCbl in sufficient quantities for thorough characterization and studies of its properties as a vitamin B_{12} analog. The crystal structure of CN-8-epiCbl has been determined. The main difference between the crystal structure of CNCbl and CN-8-epiCbl is that the *d* side chain (at C8) is "downwardly" axial in CNCbl, but pseudo-equatorial in CN-8-epiCbl. In addition, the B pyrrole ring in CN-8-epiCbl is twisted by about 5°, the axial benzimidazole moiety is tilted about 7° toward the A and D rings, and the corrin macrocycle fold angle along the Co···C10 axis (23.8°) is more severe than that in CNCbl (17.7°). Fourteen water molecules are well located in the crystal structure and four others occur at half-occupancy. The epimeric relationship between CN-8-epiCbl and CNCbl and the configuration at C8 are also evident in observed ^{1}H NMR nuclear Overhauser enhancements and differences in amide ^{1}H and ^{15}N chemical shifts at the *d* amide between CNCbl and CN-8-epiCbl. Measurements of the amide proton chemical shift thermal gradients strongly suggest the presence of a hydrogen bond in CN-8-epiCbl involving the *c* amide *syn* proton and the *d* amide carbonyl in solution. This intramolecular hydrogen bonding is not present in the crystal structure in which the *d*

* Author to whom correspondence should be addressed.

amide carbonyl is hydrogen bonded to two water molecules and the *c* amide nitrogen is hydrogen bonded to the *b* amide carbonyl oxygen of a symmetry related molecule. Comparison of the ^{13}C spectra of CNCbl and CN-8-epiCbl shows that significant chemical shift changes are not restricted to the B ring (the site of epimerization) but are more global in nature, reflecting the changes in corrin ring conformation.

The cobalamin corrin macrocycle is adorned with seven amide side chains, the *a*, *c*, and *g* acetamide side chains which project "above" the plane of the corrin ring and the *b*, *d*, *e*, and *f* propionamide side chains which project "below" the plane of the corrin ring, the last of which is elaborated into the nucleotide loop (Fig. 1). Analogues of cobalamins with altered side chains have long been of interest, particularly in studies of the interaction of coenzyme B_{12} (5′-deoxy-adenosylcobalamin, AdoCbl[1]) with AdoCbl-requiring enzymes,[2-5] and of the interaction of cyanocobalamin (vitamin B_{12}, CNCbl[1]) with intrinsic factor.[6] These analogues have included the readily available *b*-, *d*-, and *e*-monocarboxylates[7-9] and their esters[3,5] and *N*-alkyl amides,[2,4] the *c*-monocarboxylate,[10] and 13-epicobalamin,[11,12] the C13 epimer of cobalamin in which the *e* propionamide side chain projects above the plane of the corrin ring.

These studies show that alterations on a single side chain in the relative large molecule, AdoCbl, often lead to large changes in the catalytic activities of the 5′-deoxyadenosyl derivatives,[2,3] and suggest that these side chain functionalities may act as hydrogen bond donors to the enzyme active sites.[13] Recent studies of the effects of axial nucleotide coordination on the thermal homolysis of the carbon–cobalt bond of benzylCbl and neopentylCbl[14] have also led to the conclusion that the thermal motion of the corrin side chains plays a role in the entropic activation of the Co—C bond for homolysis, a reaction which closely mimics the activation of AdoCbl by AdoCbl-requiring enzymes.[15,16] Furthermore, the substantial entropic stabilization of the thermolysis of benzylCbl and neopentylCbl on binding to a haptocorrin from chicken serum[17] has suggested that the association of Cbls with haptocorrin involves extensive side chain amide hydrogen bonding, and that such interactions severely decrease the side chain thermal motion of haptocorrin-bound cobalamins. Thus, side chain steric effects may well be important in the enzymatic acti-

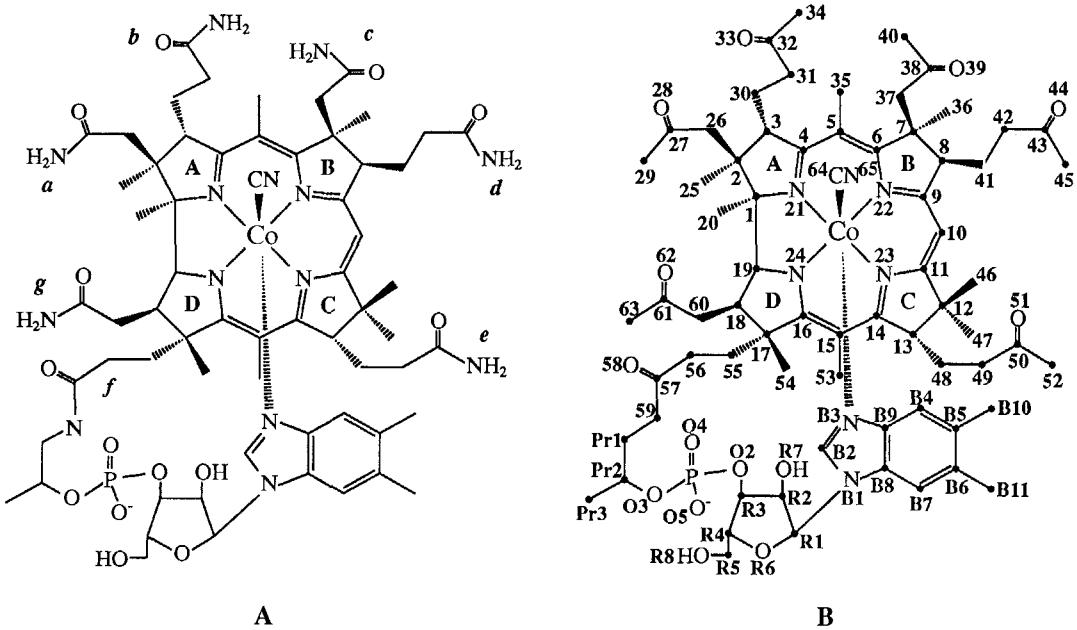

Fig. 1. Structure (A) and numbering scheme (B) for 8-epicobalamins. In the naturally occurring cobalamin system, the configuration at C8 is inverted so that the *d* propionamide side chain projects below the corrin ring.

vation of AdoCbl. We are consequently interested in exploring the carbon–cobalt bond reactivity of alkylcobalamin analogues with altered side chains.

CN-13-epiCbl has long been available from the acid-catalysed epimerization of CNCbl in anhydrous trifluoroacetic acid,[11,12] and has been characterized by X-ray crystallography.[18] In contrast, the C8 epimer of CNCbl, CN-8-epiCbl, in which the *d* propionamide side chain conformation is altered (Fig. 1) has been obtained (after amidation of its *c*-monocarboxylate derivative, CN-8-epiCbl-*c*-COO^-) as one of a number of minor products from the reduction of CNCbl-*c*-lactone with borohydride.[19] This derivative, which displayed 10% of the activity of CNCbl in a bioassay, was characterized only by its CD spectrum, which was shown to be different from that of CNCbl. As part of our study of the importance of corrin ring side chains in Co—C bond homolysis, we have reexamined and improved the synthetic procedure for CN-8-epiCbl and characterized this derivative by FAB MS, X-ray crystallography, and complete assignment of its ^1H, ^{13}C, and amide ^{15}N NMR spectra.

EXPERIMENTAL

Reagents

CNCbl was from Roussel Corp. Chloramine-T, sodium borohydride (powdery and granular), and ammonium chloride were from Aldrich. 1-Ethyl-3-(3-dimethylaminopropyl)carbodiimide hydrochloride (ECDI[1]) was from Sigma. Analytical and semipreparative HPLC was carried out as described previously.[20,21]

Synthesis

CNCbl-c-*lactone* (**2**). To a solution of CNCbl (5 g, 3.69 mmol) in 350 cm^3 of H_2O was added 5 cm^3 of conc. HCl, followed by a solution of chloramine-T (1 g, 4.43 mmol, 1.2 equiv.) in 100 cm^3 of H_2O over a 2 h period at room temperature. The cobalt corrinoids were then absorbed onto a column of Amberlite XAD-2 and washed with H_2O. The product was eluted with 25% aqueous acetonitrile, and the eluant was concentrated to give dark red crystals in 90% yield (4.48 g). UV: λ (log ε) 552 (3.96), 521 (3.92), 358 (4.48), 278 (4.16). FAB MS *m/z*: calc. (for CNCbl-*c*-lactone + H^+) 1355.4, obs. 1355.8. The ^{13}C NMR spectrum was tentatively assigned by analogy with that of CNCbl.[22,23]

CN-8-epiCBL-*c*-COO^- (**4**). CNCbl-*c*-lactone (**2**, 0.9 g, 0.67 mmol) was dissolved in 1 l of water and deoxygenated by argon purge for 1 h. The solution was heated to 60°C in a water bath, and $NaBH_4$ (7 g, 185 mmol, granular) was added in two portions at 5 min intervals. The reaction mixture was stirred for 30 min at 60°C, and then cooled to room temperature. KCN (0.5 g) was added, followed by glacial acetic acid (5 cm^3), and the solution was stirred for another 30 min. The reaction mixture, which contained 37% CNCbl-*c*-COO^- and 21% CN-8-epiCbl-*c*-COO^- by HPLC, was desalted on a column of Amberlite XAD-2 as above. CN-8-epiCbl-*c*-COO^-, which eluted slightly later than CNCbl-*c*-COO^-, was separated by semipreparative HPLC, using pH 6.5 ammonium phosphate buffer,[20,21] in 19% yield. UV: λ (log ε) 552 (3.95), 516 (3.90), 361 (4.47), 278 (4.30). FAB MS *m/z*: calc. (for CNCbl-*c*-COOH + H^+) 1357.4, obs. 1357.9. The ^{13}C NMR spectrum was tentatively assigned by analogy with that of CN-8-epiCbl (*vide infra*).

CN-8-epiCbl (**3**). CN-8-epiCbl-*c*-COO^- (**4**, 150 mg, 148 μmol) was dissolved in 120 cm^3 of a 4 M solution of NH_4Cl, the pH of which had been adjusted to 5.5 with HCl. 1-Ethyl-3-(3-dimethylamino)propylcarbodiimide (ECDI,[1] 0.75 g) was added to the solution, and the pH was readjusted to 5.5 with HCl as necessary. After stirring at room temperature for 12 h, the reaction mixture was desalted on a column of Amberlite XAD-2 as above. The amidated product was purified by semipreparative HPLC and obtained in 80% yield (120 mg). UV: λ (log ε) 552, (3.93), 520 (3.86), 360 (4.43), 276 (4.18). FAB MS *m/z*: calc. (for CN-8-epiCbl + H^+) 1356.4, obs. 1355.9.

Spectroscopy

UV–visible spectra were recorded on a Cary 219 spectrophotometer. One dimensional ^1H and ^{13}C NMR spectra of intermediates were obtained in D_2O solution containing TSP as an internal chemical shift standard on a GE QE 300 NMR spectrometer. Two-dimensional NMR spectra of CN-8-epiCbl in D_2O were obtained on a Bruker AMX 600 NMR spectrometer. For these experiments, a sample of CN-8-epiCbl was dissolved in 99.8% D_2O and evaporated to dryness four times to replace exchangeable protons with deuterons. The exchanged, dry solid, along with TSP to provide an internal reference, was dissolved in "100%" D_2O to provide a 12 mM sample.

Data for the double quantum-filtered phase-sensitive COSY experiment were collected at 600.141 MHz using a 2048 × 512 data matrix and 16 scans per t_1 value, preceded by 64 dummy scans, and a 1.0 s presaturation pulse for solvent suppression. The sweep width was 6579 Hz in both dimensions. The data matrix was zero filled to 2048 × 2048 and

apodized with a $\pi/3$ shifted sine function. The hypercomplex homonuclear Hartmann–Hahn (HOHAHA) experiment[24–26] was carried out and processed similarly using a 70 ms mixing time. The spin-locked NOE (or rotating-frame Overhauser enhancement spectroscopy, ROESY) experiment[27,28] utilized a 2048×512 data matrix with 32 scans per t_1 increment preceded by 32 dummy scans and a 1.0 s presaturation pulse for solvent suppression. The sweep width was 6579 Hz in both dimensions and the mixing time was 300 ms. The data were zero filled to 2048×2048 and apodized with a $\pi/2$ shifted sine function. The spectra were plotted in two colours to show the difference between positive contours (due to direct NOEs) and negative contours (due to relayed NOEs and Hartmann–Hahn artefacts). The ^{1}H-detected heteronuclear multiple-quantum coherence (HMQC) experiment[29–31] was conducted at 150.921 and 600.141 MHz using 30,183 Hz and 6579 Hz sweep widths in the F1 and F2 dimensions, respectively. Data were collected into a 2048×512 matrix using 16 scans per t_1 increment preceded by 64 dummy scans and a 1.0 s presaturation pulse for solvent suppression. The F1 dimension was zero filled to 1024 and the data in both dimensions were processed with a $\pi/2$ shifted sine function. Data for the ^{1}H-detected multiple-bond heteronuclear multiple-quantum coherence (HMBC) experiment[32,33] were collected similarly but using 80 scans per t_1 increment. These data were apodized with a $\pi/2$ shifted sine function in both dimensions.

The inverse-detected ^{1}H, ^{15}N HMQC spectra were obtained on a Bruker AMX 300 NMR spectrometer operating at 300.136 and 30.415 MHz. A 12 mM sample of CN-8-epiCbl in DMSO-d_6 contained TSP as an internal ^{1}H chemical shift reference. ^{15}N chemical shifts were referenced to external CH_3NO_2 but are reported relative to $NH_3(l)$ ($\delta_{CH_3NO_2} = 380.23$ ppm[34]). Data were collected into a 512×256 data matrix using sweep widths of 3623 (^{1}H) and 3042 Hz (^{15}N), and 1026 scans were collected per t_1 increment (138 μs). The data were apodized using Gaussian multiplication with -5 Hz line broadening in both dimensions. The NOESY spectrum of this sample was also obtained on a Bruker AMX 300 NMR spectrometer. Data were collected into a 2048×256 data matrix with a sweep width of 3623 Hz using 128 scans and a total mixing time of 600 ms. The data were apodized with a shifted sine bell function of 90°. Amide ^{1}H chemical shift thermal gradients were measured on the same sample using a GE QE 300 NMR spectrometer from a series of one-dimensional ^{1}H spectra taken at 5°C increments between 20 and 55°C.

X-ray crystallography

Deep wine-red to scarlet crystals of CN-8-epiCbl were grown by slow evaporation of an aqueous solution at room temperature. A prismatic specimen was cut to size while in contact with the saturated aqueous solution. The crystal, with dimensions of $0.25 \times 0.45 \times 0.30$ mm, was wedged in a 0.3 mm glass capillary tube with the saturated mother liquor and sealed from the atmosphere with silicone grease. All measurements were made using a Siemens P3 diffractometer, with Mo-K_α radiation (wavelength 0.71073 Å) at 20°C.

A survey of reflection intensities showed that the specimen diffracted to below 1.2 Å resolution, and 20 well-centred reflections with $2\theta > 20°$ gave cell constants in the orthorhombic system: $a = 14.923(4)$, $b = 17.290(5)$, $c = 32.447(7)$ Å, $V = 8370.8(39)$ Å^3. Cell volume was roughly consistent with four complexes per cell with perhaps 10–20 waters. A total of 6085 reflections was collected by omega scans from $2\theta = 3.5$ to 45.0° with three standard reflections monitored every 50 reflections. About one in ten reflections were observed at $I > 2\sigma_I$ in a shell from 45.0 to 52.5°, and an additional 2824 reflections were collected in this range. In all, 8909 unique reflections were collected over a period of 70 h in the octant over indices: $h = 0$–16, $k = 0$–21, $l = 0$–40. After correction for Lorentz and polarization effects, a correction was applied for deterioration which occurred late in the data collection. An empirical absorption correction was later applied, maximum/minimum transmission = 0.96, 0.16. Systematic absences ($h00$, h odd; $0k0$, k odd; $00l$, l odd) were consistent with space group $P2_12_12_1$. The location of the cobalt and phosphorus atoms were discovered by application of the Patterson function in SHELXS.[35] Several cycles of Fourier calculation revealed all the non-hydrogen atoms in the complex. Refinement of the positions and isotropic vibrational amplitudes for the non-hydrogen atoms in the complex converged at $R = 0.14$ for 4105 reflections with $I > 2\sigma_I$ for 409 parameters, with the identities of the terminal amide oxygens and nitrogens deduced from the bond distances. Oxygens from 16 waters were located in a difference Fourier map. These seem to consist of 14 ordered waters plus two sets of two half-occupancy waters in the same vicinity. Amide side chains seemed ordered with the exception of the β-carbon (C42) in the *d* propionamide at C8 which was found with equal likelihood in either of two gauche positions between the α-carbons and carbonyl carbons of its chain.

Gradually, anisotropic vibrational amplitudes

were introduced for all non-hydrogen atoms including water oxygens as the refinement proceeded by blocked least-squares. A computer program, SHELXL-93,[36] was employed to minimize the F^2 differences. Hydrogen atoms were placed in calculated positions where these were unambiguous, and in positions determined by examining difference Fourier maps for others. Hydrogen atom positions were not refined, nor were water hydrogens included. Some of the terminal amides gave anisotropic vibrational parameters suggestive of small local disorders, but a number of trials failed to find more satisfactory models. Stable refinement of one amide carbonyl (C61), found near the disordered solvent region, required an isotropic vibrational factor. A small extinction correction was applied, which refined to 0.00027(7). The model converged with $R_1 = \Sigma \| F_{obs}| - |F_{calc} \| / \Sigma |F_{obs}| = 0.0521$ (on F, for values of 2852 $F > 4\sigma_F$), $wR_2 = \{\Sigma[w(F_{obs}^2 - F_{calc}^2)^2]/\Sigma[w(F_{obs}^2)^2]\}^{1/2} = 0.1260$ on F^2 for all 8909 data. Flack's analysis supports the absolute configuration of the model.[37]

RESULTS

Synthesis of CN-8-epiCbl

CN-8-epiCbl was synthesized by a modification of the route of Rapp and Oltersdorf[19] as shown in Scheme 1. This route involves the oxidation of CNCbl (**1**) to the *c*-lactone (**2**) followed by reduction of the lactone with granular borohydride to give a pair of *c*-monocarboxylates epimeric at C8 (**3** and **4**). Amidation of the CN-8-epiCbl-*c*-COO^- (**4**) generates the CN-8-epicobalamin (**5**).

The well characterized CNCbl-*c*-lactone has been obtained under acidic, oxidative conditions using chloramine-T or bromine water,[10] or *N*-bromosuccinamide in 0.5 M acetic acid.[38] In the original method of Bonnett *et al.*,[10] chloramine-T was mixed with CNCbl, followed by addition of hydrochloric acid to give the lactone in 23% yield. We have found that slow addition of the acid catalyst improves the yield of lactone to 60–70%. The main side product of this reaction, 10-Cl-CNCbl-*c*-lactone, results from facile chlorination of the lactone product at the corrin ring carbon, C10.[10] We consequently reasoned that chlorination of the lactone could be minimized by avoiding conditions in which an excess of chloramine-T was present. Indeed, when the order of addition of the reagents was reversed, so that solution of chloramine-T was added dropwise to a mixture of CNCbl and HCl over a 2 h period, the yield of lactone formation was improved from 23 to 90%.

The key step in the synthesis of CN-8-epiCbl is the reductive epimerization of the lactone. Rapp and Oltersdorf[19] originally reported that reduction of the lactone with $NaBH_4$ in water afforded CN-8-epiCbl-*c*-COO^- in 8% yield along with CNCbl-

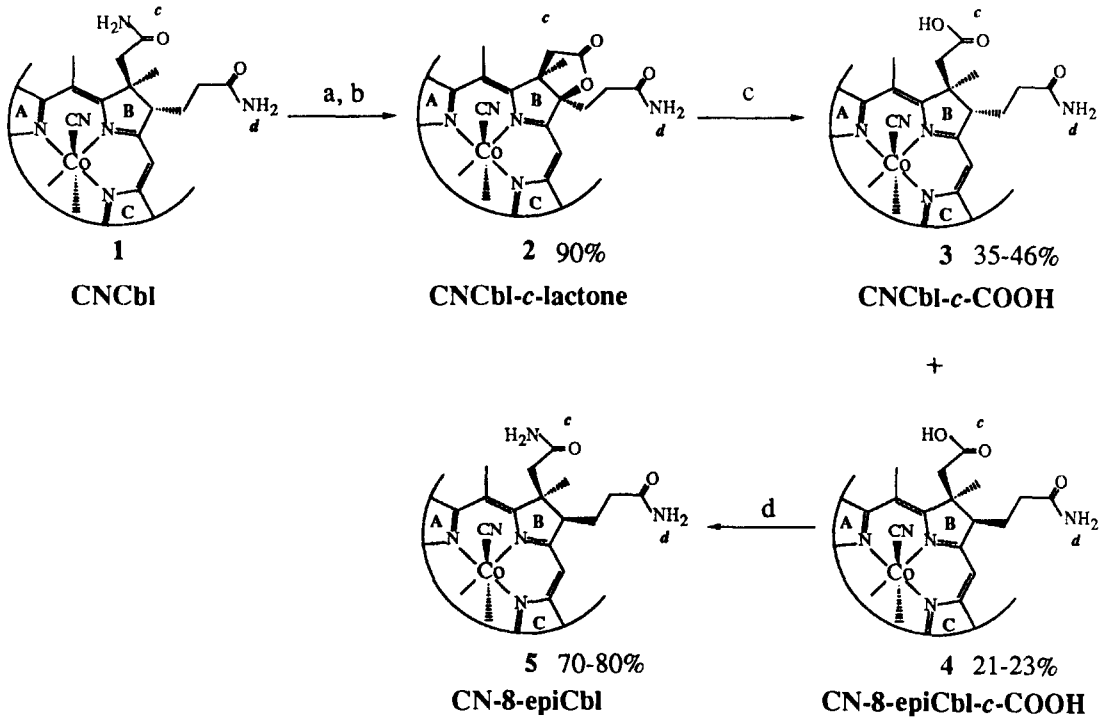

Scheme 1. (a) HCl; (b) chloramine-T; (c) $\Delta + NaBH_4$; (d) NH_4Cl/ECDI.

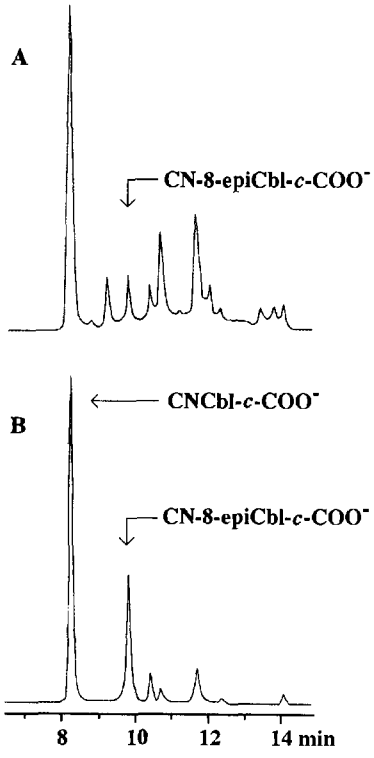

Fig. 2. High performance liquid chromatograms of the reaction mixtures resulting from reduction of CNCbl-*c*-lactone in water using sodium borohydride powder at room temperature (A) and with granular sodium borohydride at 60°C (B).

c-COO^-. Using the reported method, we obtained a mixture containing at least eight components (Fig. 2A), with CN-8-epiCbl-*c*-COO^- in 4% yield at best. Because of the low yield and the difficulty in separating the desired product from such a complicated reaction mixture, attempts were made to find conditions that would improve the result. We found that by raising the reaction temperature to 60°C, the yield of CN-8-epiCbl-*c*-COO^- was marginally improved to 5–7%. However, when granular $NaBH_4$, instead of $NaBH_4$ powder, was used at 60°C in water, the reaction was cleaner (Fig. 2B), and the yields in four separate preparations ranged from 21 to 23%, by HPLC integration. The two diastereomeric products were readily separable by semipreparative HPLC.

Amidation of cobalamin carboxylates in good yield requires reaction with an efficient coupling reagent. Because Cbls are only soluble in strongly polar solvents such as water, methanol, and DMSO, the choice of coupling reagents is somewhat limited. Among the coupling reagents tried (including dicyclohexylcarbodiimide in H_2O/CH_3CN and ethyl chloroformate in DMSO), 1-ethyl-3-(3-dimethylamino)propyl carbodiimide gave the best results for CN-8-epiCbl (70–80%).

X-ray structure

Cyano-8-epicobalamin hexadecahydrate crystallizes in the orthorhombic system, space group $P2_12_12_1$. All bond lengths and angles were found to be consistent with the established CNCbl structure[39] and have chemically reasonable values. Table 1 shows the details of the crystal data and structure refinement. Selected bond lengths, bond angles, and torsion angles are given in Table 2. (The atomic coordinations are given in Table S2, anisotropic temperature factors are given in Table S3, all bond distances and angles between adjacent non-hydrogen atoms are given in Table S4, calculated hydrogen atom coordinates are given in Table S5, and intermolecular contacts are described in Table S6, available as supplementary materials.)

The central cobalt atom is pseudo-octahedral, coordinated to the four equatorial corrin nitrogens, a nitrogen from the axial Bzm nucleotide and the cyanide carbon atom. Distortions from octahedral geometry are readily evident from the inner sphere bond distances and angles which are close to those of CNCbl (Table 2). Overall, the structure is quite similar to that of CNCbl.[39] However, the *d* propionamide side chain at C8, which occupies a "downward" axial position in CNCbl, is pseudo-equatorial in CN-8-epiCbl. The only disorder found in the molecule is at the β-carbon (C42) for this side chain which occurs at two positions with equal occupancy. Each position completes one of two alternate gauche arrangements of the propionamide chain, C8—C41—C42—C43, and the bond distances are normal for each.

All peripheral N and O atoms except the ribose ring oxygen and the carbon-bonded phosphodiester oxygens engage in hydrogen bonding. However, no intramolecular hydrogen bonds occur, and contact between the molecules is minimal, with only three of 15 hydrogen bonding contacts not involving

Table 1. Crystal data for CN-8-epiCbl

Empirical formula	$C_{63}H_{75}CoN_{14}O_{14}P \cdot 16H_2O$
Formula weight	1630.53 (including H_2O)
Temperature (K)	293(2)
λ (Mo-K_α) (Å)	0.71073
Space group	$P2_12_12_1$
a (Å)	14.923(4)
b (Å)	17.290(5)
c (Å)	32.447(7)
V (Å^3)	8372(4)
Z	4
Crystal size (mm^3)	$0.25 \times 0.45 \times 0.30$
D (g cm^{-3})	1.294

Table 2. Selected bond lengths, bond angles, and torsion angles for CN-8-epiCbl

	CN-8-epiCbl	CNCbl
Bond length (Å)		
Co—C64	1.911(10)	1.92
Co—B3(N)	2.015(6)	1.97
Co—N21	1.847(6)	1.80
Co—N22	1.894(6)	1.92
Co—N23	1.902(6)	1.86
Co—N24	1.872(6)	1.87
C64—N65	1.133(9)	1.11
C3—C4	1.516(9)	1.57
C4—N21	1.307(8)	1.39
C4—C5	1.405(9)	1.33
C5—C6	1.384(9)	1.50
C5—C35	1.538(7)	1.61
C9—C10	1.399(10)	1.60
C10—C11	1.367(10)	1.28
C11—C12	1.484(10)	1.58
C14—N23	1.398(8)	1.52
C16—C17	1.512(10)	1.42
C17—C18	1.559(10)	1.62
C18—C19	1.518(9)	1.60
C19—N24	1.490(8)	1.54
Bond angle (°)		
C64—Co—B3(N)	177.5(3)	174
N65—C64—Co	178.3(9)	176
N21—Co—N22	89.4(3)	89
N22—Co—N23	96.1(3)	96
N23—Co—N24	91.1(3)	92
N21—Co—N24	83.5(3)	84
N21—Co—C64	88.9(3)	87
N22—Co—C64	87.9(3)	87
N23—Co—C64	92.9(2)	91
N24—Co—C64	87.8(3)	89
N21—Co—B3(N)	91.5(3)	96
N22—Co—B3(N)	89.6(2)	88
N23—Co—B3(N)	86.9(3)	87
N24—Co—B3(N)	94.7(3)	97
C6—N22—Co	127.1(5)	132
C9—C10—C11	124.9(8)	121
C10—C11—C12	122.8(8)	118
C15—C16—C17	128.4(7)	124
N24—C16—C17	110.5(7)	115
N24—C19—C18	102.1(6)	99
C18—C19—C1	123.5(7)	127
B2—B3(N)—Co	124.3(6)	117
B9—B3(N)—Co	132.1(5)	139
Torsion angle (°)		
C1—C2—C3—C4	−33	−40
C2—C3—C4—C5	−157	−153
C3—C4—C5—C6	−165	−159
C4—C5—C6—C7	174	171
C5—C6—C7—C8	−153	−165
C6—C7—C8—C9	−32	−22
C7—C8—C9—C10	−145	−151
C8—C9—C10—C11	172	−179
C9—C10—C11—C12	−165	−165
C10—C11—C12—C13	−164	−169
C11—C12—C13—C14	−21	−29
C12—C13—C14—C15	−167	−163
C13—C14—C15—C16	−172	−171
C14—C15—C16—C17	−172	−173
C15—C16—C17—C18	−168	−167
C16—C17—C18—C19	−31	−29
C17—C18—C19—C1	155	153
C18—C19—C1—C2	90	93
C19—C1—C2—C3	138	145
C5—C6—N22—C9	172	179
C8—C7—C6—N22	26	17
C7—C8—C9—N22	31	31
N23—C11—C12—C46	147	147
N23—C11—C12—C47	−95	−96
C14—C13—C12—C46	−152	−152
C14—C13—C12—C47	90	90

crystallized solvent. Eighteen water oxygens have been located in the unit cell, 14 of which are apparently ordered, while four are half-occupancy with either O(15W) and O(17W) or O(16W) and O(18W) present. These water molecules form 12 hydrogen bonds to amide, phosphate, ribose, and cyanide heteroatoms. Three additional hydrogen bonds occur between oxygens and nitrogens of symmetry related molecules.

^{1}H *and* ^{13}C *NMR*

In order to complete the characterization of CN-8-epiCbl, previously characterized only by its CD spectrum[19] and to make a comparison of the crystal and solution structures, as well as to provide information as to how epimerization at corrin ring C8 affects the overall ^{13}C chemical shifts of CNCbl, we have completely assigned the ^{1}H and ^{13}C NMR spectra of CN-8-epiCbl using modern 2D NMR methods. The COSY spectrum (not shown) and the homonuclear Hartmann–Hahn (HOHAHA) spectrum (Fig. 3) were used to identify the ribose, isopropanolamine, C3—C30—C31, C8—C42—C43, C13—C48—C49, and C19—C18—C60 spin systems. The ribose spin system could be readily assigned since the only downfield doublet in the ^{1}H spectrum (6.41 ppm) could be confidently assigned to the R1 proton (Fig. 1). Similarly, the Pr3 methyl resonance can be identified (1.33 ppm) as the only three proton doublet resonance in the ^{1}H spectrum, since Pr3 is the only spin-coupled methyl group in the molecule (Fig. 1). Absolute assignment of the

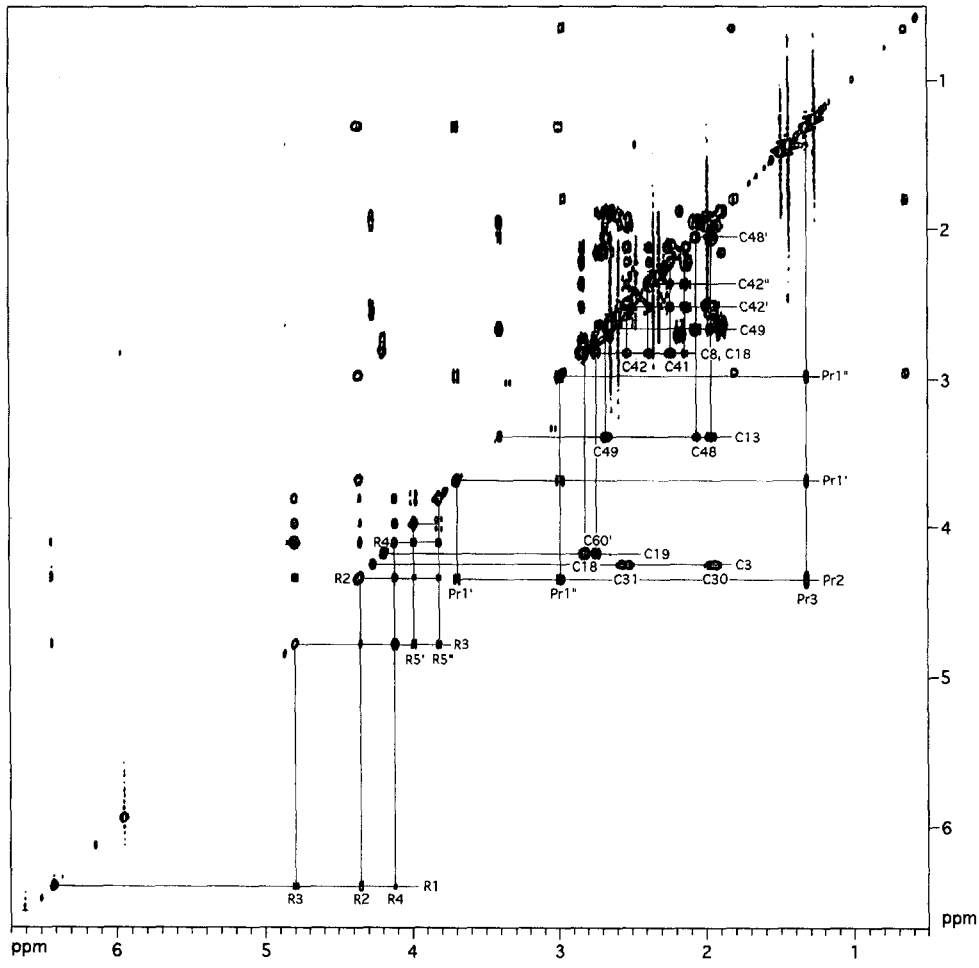

Fig. 3. Two-dimensional homonuclear Hartmann–Hahn (HOHAHA) spectrum of CN-8-epiCbl in D_2O showing extended spin–spin couplings in the R1—R5, Pr1—Pr2—Pr3, C3—C30—C31, C8—C41—C42, C13—C48—C49, and C19—C18—C60 spin systems.

other spin systems requires further information. In both the COSY and HOHAHA spectra, four methylene protons show correlations only among themselves. These must represent the C55 and C56 methylene protons, since these are the only adjacent methylenes not coupled to a ring proton in the molecule (Fig. 1). However, distinguishing the C55 and C56 ^1H and ^{13}C resonances requires information from the HMQC and HMBC spectra.

As has been the case with several 5′-deoxyadenosylcobalt corrinoids,[32,40] the crosspeaks in a standard absorption mode NOE (NOESY) spectrum[41,42] were relatively weak, suggesting that the rotational correlation time for CN-8-epiCbl is close to the reciprocal of the Larmor frequency at this field strength (14.1 T). However, the spin-locked NOE experiment (ROESY), in which crosspeaks are always positive and increase in intensity with slower molecular motion,[27] gave good spectrum as shown in Fig. 4. Since the ROESY experiment generates crosspeaks between protons which are close ($\leqslant 4$ Å) to each other in space via the nuclear Overhauser enhancement, it can be used to confirm the assignment of spin systems including a ring proton and attached methylenes, as well as to assign the resonances of protons which are not coupled to any other protons. For instance, the downfield proton resonance at 5.93 ppm, which correlates to a carbon resonance at 93.95 ppm in the HMQC spectrum (see below), can confidently be assigned to C10.[22,23,32,40,43–46] This resonance shows crosspeaks to resonances which can be assigned to C8, C41′, C42′, C42″,[1] C46, and C47, the last two of which have crosspeaks with the C13 resonance. Most importantly, strong NOE crosspeaks are seen between the C41″ proton and C37′ and C37″ and between the C8 proton and the B4 proton, but no NOEs are seen between the C8 proton and the C37 protons as is commonly the case in normal cobalamins.[32,40,43–47]

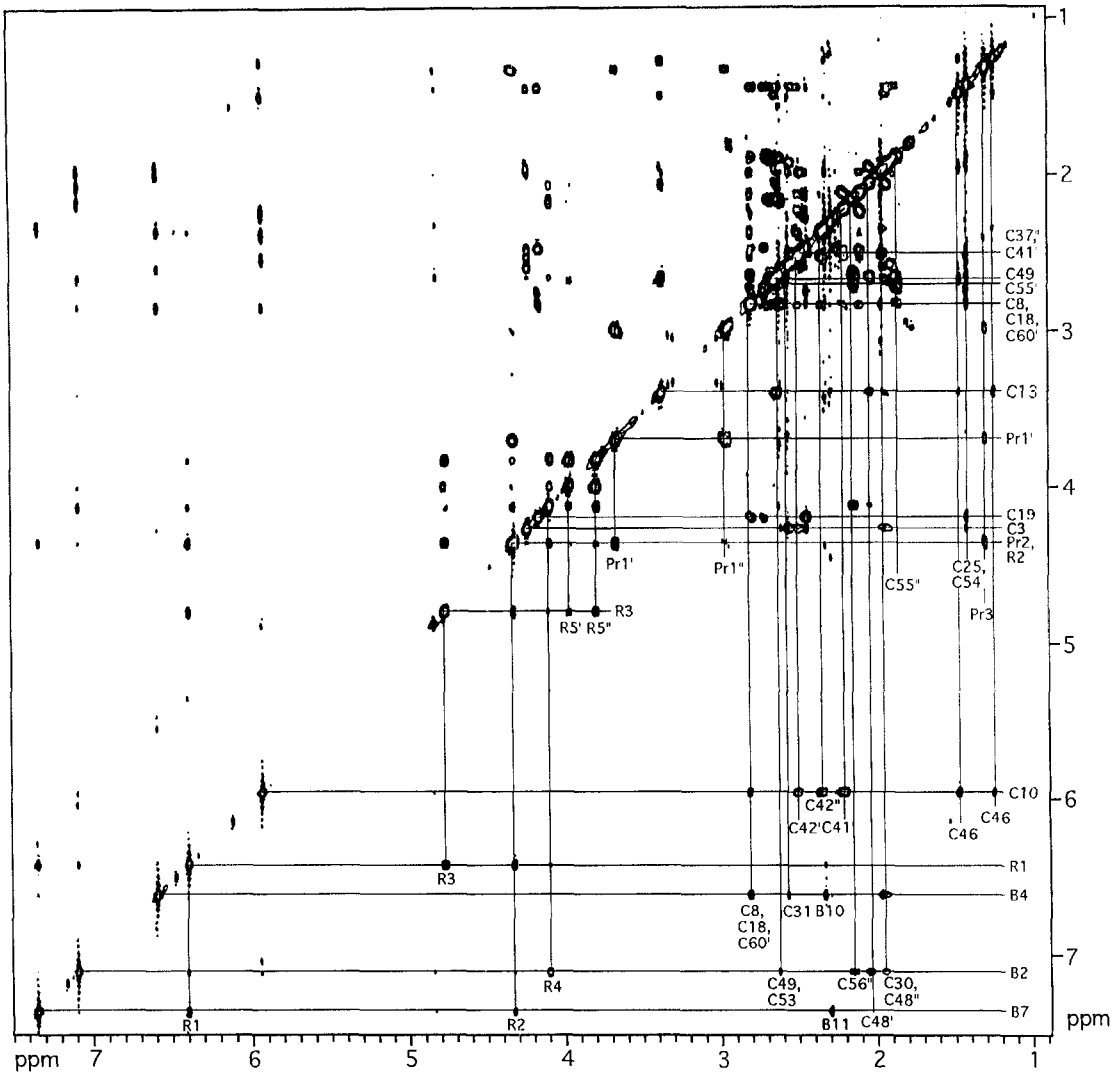

Fig. 4. Spin-locked NOE (or rotating-frame Overhauser enhancement spectroscopy, ROESY) spectrum of CN-8-epiCbl in D_2O showing various through space connectivities.

Following assignment of the ^1H spectrum, the ^{13}C spectrum was assigned using the HMQC and HMBC heteronuclear correlation experiments. The former experiment, in which crosspeaks arise only between carbons and their directly attached protons, permits unambiguous assignment of the protonated carbons except in those instances where two carbon atoms are bonded to magnetically equivalent hydrogens. The axial nucleotide resonances were assigned largely from the HMBC spectrum based on the expectation that the three-bond H—C couplings in such an aromatic system will be larger than the two-bond H—C coulings[48] as originally discussed by Summers *et al.*[32]

One of the most challenging aspects of the assignment of the NMR spectra of cobalt coorinoids is the assignment of the downfield ^{13}C resonances, all of which are unprotonated, since, for example in the present case, the resonances of 10 carbons (the seven carbonyl carbons and C4, C9, and C11) occur in a narrow range of 4.9 ppm. Often this spectral crowding, in addition to the spectral overlaps in the ^1H spectrum, has required observation of numerous HMBC sub-spectra in order to sort out the H—C correlations in this region of the spectrum.[40,49] Figure 5 shows, however, that at 600 MHz there is sufficient spectral dispersion and sensitivity to assign completely this region of the spectrum unambiguously simply by inspection of the HMBC 2D spectrum. The final ^1H and ^{13}C assignments are given in Table 3.

Amide ^1H and ^{15}N NMR

In D_2O, the amide protons of cobalamins exchange rapidly with solvent. However, in DMSO-

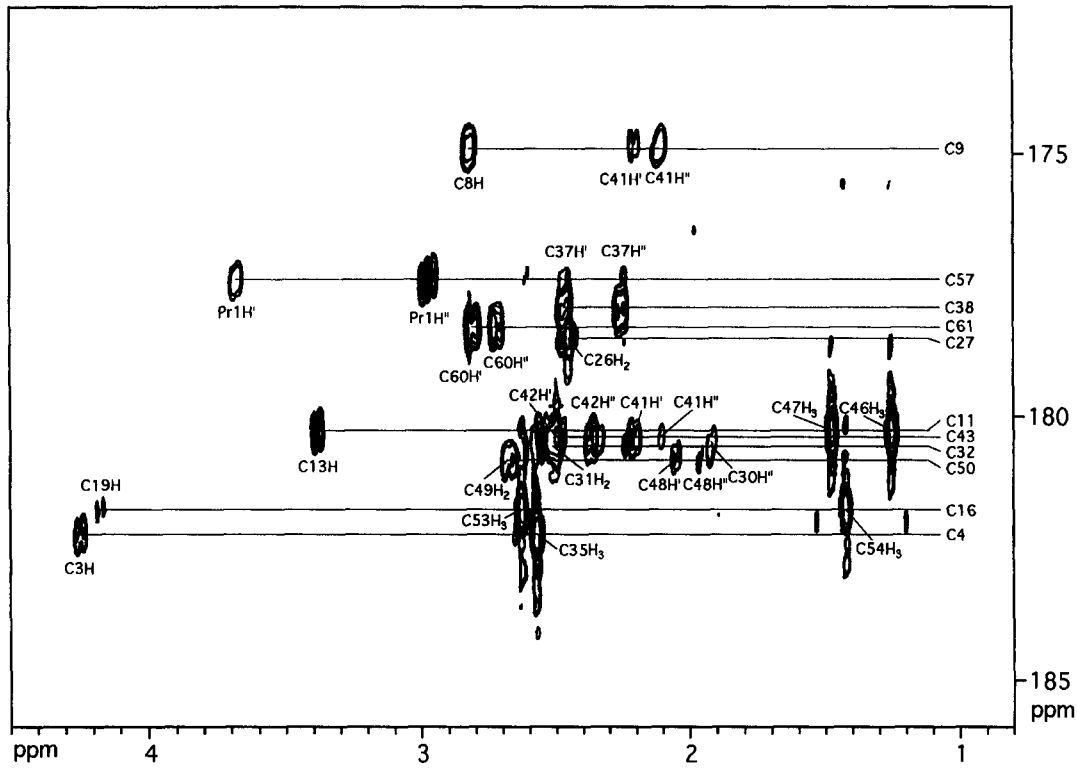

Fig. 5. Portion of the HMBC spectrum of CN-8-epiCbl showing the long range C—H correlations involving the carbonyl carbons and corrin ring C4, C9, C11 resonances. Additional correlations (not shown) occur between C10H and C9 and C11.

d_6 these protons persist, and can be used to observe the amide ^{15}N resonances by polarization transfer[50,51] or by inverse detected HMQC.[47,51,52] Figure 6 shows such a ^1H, ^{15}N HMQC spectrum for CN-8-epiCbl in DMSO-d_6 at 30°C. The spectrum consists of seven ^{15}N resonances, six of which show crosspeaks to two protons (i.e., the amide *anti* and *syn* protons). We assume[47] that the downfield resonance of each pair is due to the *anti* proton and the upfield resonance is due to the *syn* proton as is the case for other amides.[53–57] The seventh resonance has only a single crosspeak and can consequently immediately be assigned to the *f* amide, the only substituted amide in the molecule. In order to assign unambiguously the remaining amide ^{15}N resonances, a NOESY spectrum of the same sample was recorded using a long mixing time of 600 ms. Under these conditions, as shown in Fig. 7, numerous crosspeaks can be seen between the amide hydrogens and those of the corrin ring and its side chains. In order to assign correctly these crosspeaks, the complete NOESY spectrum of CN-8-epiCbl in DMSO-d_6 was assigned in analogy to the ROESY spectrum of Cn-8-epiCbl in D_2O. (The resulting ^1H NMR assignments of CN-8-epiCbl in DMSO-d_6 and the NOE correlations upon which they are based are summarized in Table S8, available as supplementary material.) With these assignments in hand, all of the amide proton resonances could be assigned from their crosspeaks in the NOESY spectrum with the exception of the amide proton resonance at 7.23 ppm for which no crosspeaks were observed. This resonance was assigned to the *d'* proton by default. The assignments of the amide ^1H and ^{15}N resonances of CN-8-epiCbl are given in Table 4 along with those of CNCbl[47] for comparison. As can be seen in Table 4, the only ^{15}N chemical shift which differs significantly between these epimers is that of the *d* amide, which is shifted 1.6 ppm upfield in CN-8-epiCbl. In addition, only the *c* and *d* amide protons of CN-8-epiCbl have chemical shifts significantly different from those of CNCbl. The ^{15}N and ^1H chemical shift differences of the *d* amide confirm that it is in different environments in the two epimers, while the chemical shift differences for the *c* amide protons suggest that there may be an interaction between the *c* and *d* amides in CN-8-epiCbl.

In order to determine if there is a hydrogen bonding interaction between the *c* and *d* amides in CN-8-epiCbl, the amide ^1H chemical shift thermal gradients, $-(\Delta\delta/\Delta T)$, were determined for CN-8-epiCbl

Table 3. ^{1}H and ^{13}C NMR chemical shift assignments for CN-8-epiCbl[a]

Atom	$\delta^{13}C$ (ppm)	$\delta^{1}H$ (ppm)	$\Delta\delta^{13}C$[b] (ppm)	Atom	$\delta^{13}C$ (ppm)	$\delta^{1}H$ (ppm)	$\Delta\delta^{13}C$[b] (ppm)
C53	17.80	2.65	−0.08	R5	63.06	3.98, 3.81	−0.04
C54	18.30	1.45	0.12	R2	71.39	4.35	0.05
C35	18.44	2.60	−0.48	Pr2	75.53[c]	4.35	−0.01
C25	19.32	1.45	0.05	R3	75.73[d]	4.79	−0.16
Pr3	21.64	1.33	−0.04	C19	77.67	4.16	−0.19
C47	21.66	1.50	0.12	R4	84.67[e]	4.11	−0.08
C20	21.69	0.42	0.09	C1	87.58		0.08
B11	21.96	2.32	−0.01	R1	89.44	6.41	0.17
B10	22.59	2.36	−0.12	C10	93.95	5.93	3.52
C41	22.90	2.24, 2.13	5.63	C15	107.00		−0.35
C36	24.89	1.99	−3.29	C5	110.79		−0.71
C30	28.51	1.99, 1.93	0.02	B7	114.15	7.34	−0.01
C48	30.71	2.07, 1.96	−0.13	B4	118.27	6.60	0.75
C46	34.02	1.26	−0.16	B8	132.44		0.04
C60	34.11	2.82, 2.74	0.68	B5	136.13		−0.54
C55	34.89	2.70, 1.89	0.25	B6	137.45		0.23
C56	35.60	2.70, 1.89	−1.31	B9	139.70		−0.45
C42	36.70	2.53, 2.37	−2.46	B2	144.50	7.10	−0.10
C49	37.17	2.67	0.06	C6	165.75		2.10
C31	37.52	2.55	0.02	C14	168.56		0.02
C18	41.54	2.83	0.05	C9	174.81		1.29
C37	42.00	2.49, 2.27	3.55	C57	177.31		0.06
C26	45.25	2.46	0.16	C38	177.90		−0.03
Pr1	47.91	3.69, 2.98	0.03	C61	178.24		0.10
C2	50.00		−0.21	C27	178.39		0.07
C12	50.94		−0.25	C11	180.21		−0.77
C7	55.13		−1.11	C43	180.34		−0.62
C13	56.18	3.40	0.04	C32	180.37		0.11
C3	58.68	4.23	0.17	C50	180.68		0.11
C8	60.05	2.82	−1.80	C16	181.68		−0.22
C17	61.91		−0.16	C4	182.17		0.41

[a] In D_2O. Chemical shifts in ppm relative to internal TSP.
[b] Difference in chemical shift between CNCbl and CN-8-epiCbl.
[c] $2J_{PC} = 6.1$ Hz.
[d] $2J_{PC} = 3.5$ Hz.
[e] $3J_{PC} = 6.7$ Hz.

in DMSO-d_6 (Table 4). The chemical shifts of substituted amide protons (i.e., peptides amides) hydrogen bonded to solvent molecules in DMSO normally move upfield with increasing temperature, on the order of 4–10 × 10^{-3} ppm per °C, while intramolecular hydrogen bonding retards these chemical shift thermal gradients significantly.[58,59] Our previous studies of the chemical shift thermal gradients of the amide protons of 15 cobalt corrinoids[47,51,52] have shown that corrinoid amide protons exposed to solvent and not involved in intramolecular hydrogen bonds have $-(\Delta\delta/\Delta T) \geqslant 3.0 \times 10^{-3}$ ppm per °C, while those which are intramolecularly hydrogen bonded and shielded from solvent have $-(\Delta\delta/\Delta T) \leqslant 2.0 \times 10^{-3}$ ppm per °C.[47]

At 30°C, three of the amide protons of CN-8-epiCbl, the *b″*, *c″*, and *d″* protons, resonate at the same chemical shift (6.78 ppm, Fig. 6). As the temperature is increased, two of these resonances shifts upfield with "normal" chemical shift thermal gradients ($5.09 \pm 0.04 \times 10^{-3}$ ppm per °C) while the gradient of the third proton is substantially smaller ($1.8 \pm 0.13 \times 10^{-3}$ ppm per °C). In order to determine which of the three protons had the small chemical shift thermal gradient, ^{1}H, ^{15}N HMQC spectrum of CN-8-epiCbl in DMSO-d_6 was observed at 50°C. This spectrum (not shown) clearly showed that it is the *c″* proton that resolves from the *b″* and *d″* protons at higher temperatures and has the low chemical shift thermal gradient. This suggests that the *c* amide *syn* proton is involved in an intramolecular hydrogen bond in CN-8-epiCbl. In addi-

tion, as can be seen in Table 4, the *f* amide proton also has a reduced chemical shift thermal gradient ($0.96 \pm 0.14 \times 10^{-3}$ ppm per °C) and is presumably involved in an intramolecular hydrogen bond, as is the case in all other base-on cobalamins studied to date.[47]

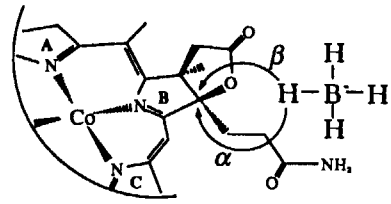

6

DISCUSSION

Reductive epimerization of CNCbl-*c*-lactone by borohydride attack at the C8 carbon of the corrin ring is the key step in the synthesis of CN-8-epiCbl. As shown in structure **6**, the attack can occur either from above the corrin ring plane, to yield CNCbl-*c*-COO$^-$ with net retention of the configuration at C8, or from below the corrin ring plane, to invert the configuration at C8 and produce CN-8-epiCbl-*c*-COO$^-$. Evidently, the lower (α) face of the corrin ring is more sterically crowded than the upper (β) face, due to the downward projecting propionamide side chains and the presence of the bulky 5,6-dimethylbenzimidazole ligand, thus favouring attack of borohydride from above the corrin ring, leading

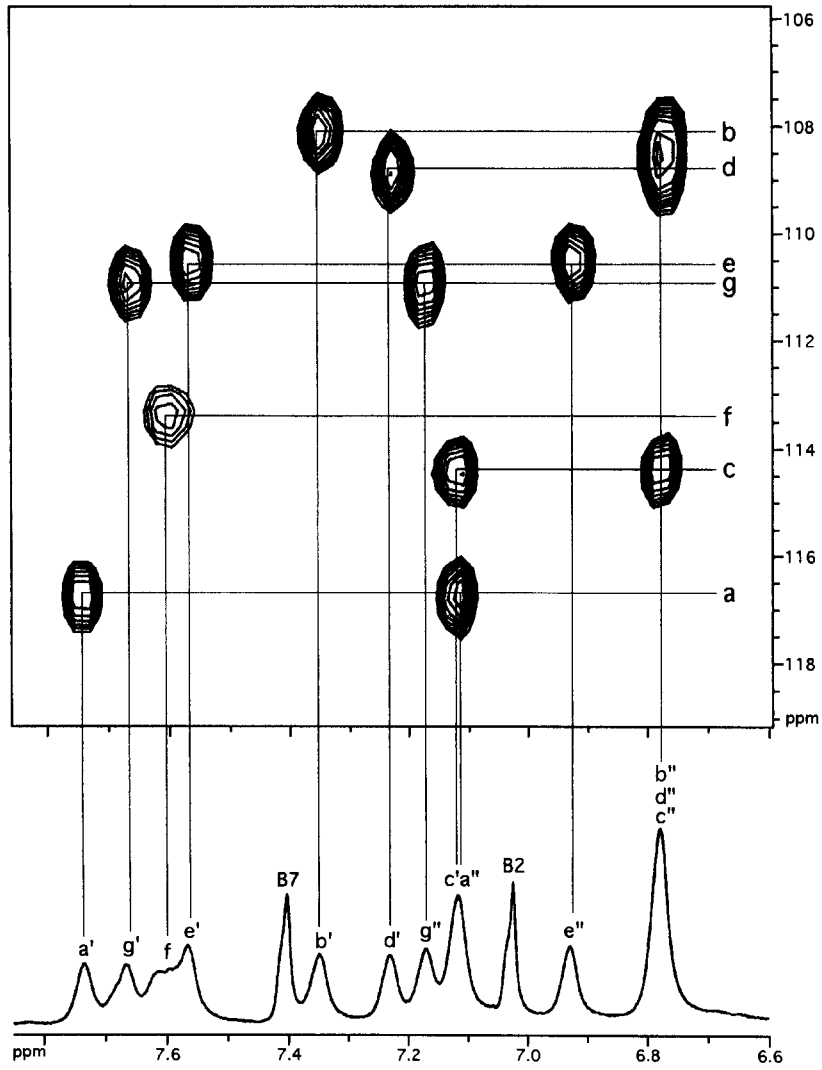

Fig. 6. The ^{1}H, ^{15}N HMQC spectrum of CN-8-epiCbl in DMSO-d_6 at 30°C. Connectivities of the amide ^{15}N resonances and their attached protons are shown using the accompanying downfield portion of the 1D ^{1}H NMR spectrum. The amide protons are designated by the side chain letter (Fig. 1) and as prime for the downfield (*anti*) proton and double prime for the upfield (*syn*) proton.

to a preponderance of CNCbl-*c*-COO^- among the products. In our hands, the reported method[19] favoured formation of CNCbl-*c*-COO^- by about 8:1 over CN-8-epiCbl-*c*-COO^-, and the net yield of the latter was only 4%. We reasoned that an increase in temperature should increase the overall reactivity and thus decrease the unfavoured steric selectivity of the reaction. This strategy proved effective since carrying out the borohydride reduction of CNCbl-*c*-lactone at 60°C improved the ratio of CNCbl-*c*-COO^- : CN-8-epiCbl-*c*-COO^- to about 5:1, and the net yield of the C8 epimer to 5–7%. What is more important in the reaction, however, was found to be the state of the sodium borohydride used. Granular $NaBH_4$ was found to be much more efficient than $NaBH_4$ powder, and the yield of CN-8-epiCbl-*c*-COO^- formation with the former at 60°C in water was found to be 21–23%, almost triple that by the original method. Apparently, powdery $NaBH_4$ decomposes too rapidly at high temperatures, as evidenced by a large amount of H_2 formation within the first few minutes after its addition, and thus has less reducing ability under these conditions.

Unlike CNCbl, whose solution is stable at mildly high temperatures, CN-8-epiCbl is thermally labile. While it is stable in neutral buffer solution at room temperature, it decomposes completely at 60°C in about 10 h, mostly forming CNCbl. This epimerization appears to be base-catalysed since in a pH 10.6 solution, CN-8-epiCbl cleanly epimerized to form CNCbl in a few hours at room temperature.

The molecular structure of CN-8-epiCbl is shown in a stereo view in Fig. 8, and in Fig. 9, superimposed at the four equatorial nitrogens (RMS deviation 0.05 Å) on the structure of CNCbl.[39] The

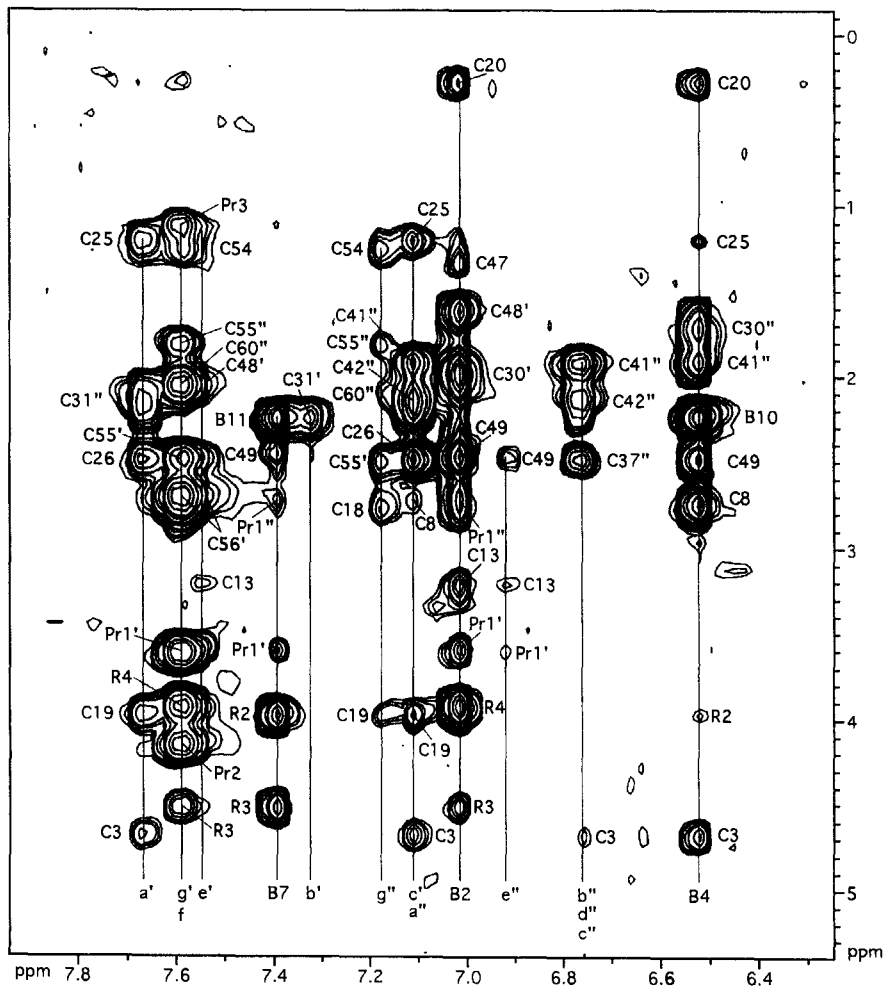

Fig. 7. Portion of the NOESY spectrum of CN-8-epiCbl in DMSO-d_6, showing the through-space connectivities between the amide and axial benzimidazole protons and other protons in the molecule, which were used to assign the ^1H, ^{15}N HMQC spectrum in Fig. 6.

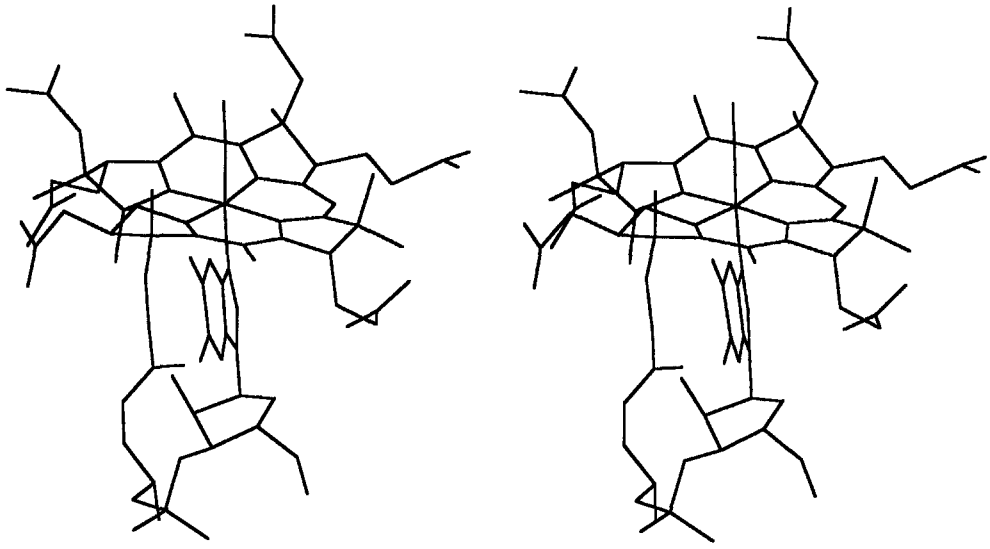

Fig. 8. Stereo view of CN-8-epiCbl crystal structure, viewed roughly along the C53 · · · C15 axis from above the corrin ring.

most important difference between the two structures is the epimerization at C8, which changes the orientation of the *d* propionamide side chain from "downward" axial to pseudo-equatorial (Fig. 9A). While disorder in the *d* side chain at C42 leads to two alternate gauche arrangements of this propionamide with equal occupancy (only one of which, C42A in Table 2, is shown in Figs 8 and 9), the *d* side chain remains pseudo-equatorial in both arrangements. In addition, the *c* acetamide can be seen (Fig. 9) to be rotated about 90° counter-clockwise (when the structure is viewed from above) about the C7—C37 bond in CN-8-epiCbl relative to CNCbl. Such differences in side chain conformation are quite common in the X-ray crystal structures of cobalt corrinoids, as shown by Glusker and coworkers' study of the structures of 13 corrinoids,[60] which show that the conformations of the *c*, *d*, and *e* side chains are more variable than the others.

As can be seen from the bond distances and bond angles in Table 2, the inner sphere geometry of CN-8-epiCbl and CNCbl are quite similar. The largest differences in bond distance occur for the Co—N (axial) bond, which is 0.05 Å longer in CN-8-epiCbl, and the Co—N23 bond, which is 0.04 Å longer in CN-8-epiCbl. However, the axial Bzm nucleotide in CN-8-epiCbl is tilted towards the A and D pyrrole rings by about 7° in CN-8-epiCbl, as can be seen in Fig. 9B. This results in a 7° increase in the Co—B3(N)—B2 bond angle and a 7° decrease in the Co—B3(N)—B9 bond angle in CN-8-epiCbl.

The largest differences in corrin ring conformation between CN-8-epiCbl and CNCbl occur at the B pyrrole ring, the site of epimerization. In CN-8-epiCbl, the B ring is twisted by about 5° with respect to its orientation in CNCbl, such that C6 and C7 are displaced above their locations in CNCbl, but C8 and C9 are displaced below, as seen in Fig. 9B. This effect leads to significant differences in a number of torsion angles in the B ring (Table

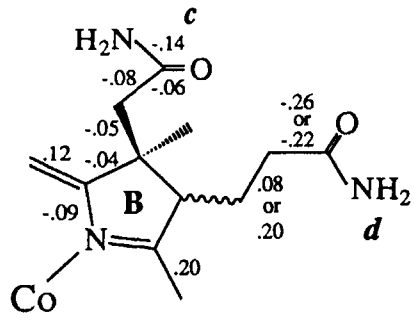

7

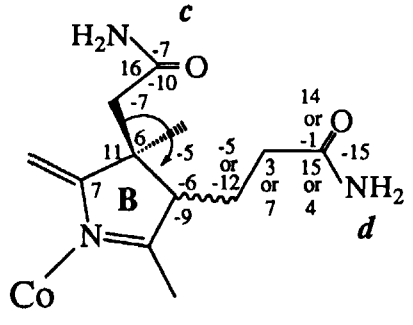

8

Table 4. Amide ^1H and ^{15}N NMR chemical shifts and ^1H chemical shift thermal gradients for CN-8-epiCbl and CNCbl[a]

	CN-8-epiCbl			CNCbl[b]		
Amide	$\delta^{15}N$ (ppm)	δ^1H (ppm)	$-(\Delta\delta/\Delta T)\times 10^3$ (ppm per °C)	$\delta^{15}N$ (ppm)	δ^1H (ppm)	$-\Delta\delta/\Delta T)\times 10^3$ (ppm per °C)
b	108.1	6.78	5.09 ± 0.04	107.9	6.76	5.14 ± 0.07
		7.35	3.85 ± 0.04		7.34	3.76 ± 0.11
d	108.8	6.78	5.09 ± 0.04	107.2	6.50	4.49 ± 0.26
		7.23	3.51 ± 0.02		6.68	4.43 ± 0.20
e	110.5	6.93	5.51 ± 0.03	110.6	6.91	5.49 ± 0.08
		7.56	3.84 ± 0.06		7.54	4.41 ± 0.07
g	110.9	7.17	5.58 ± 0.07	111.0	7.14	5.50 ± 0.08
		7.67	4.30 ± 0.16		7.64	4.54 ± 0.12
f	113.4	7.61	0.96 ± 0.14	113.4	7.60	0.99 ± 0.25
c	114.4	6.78	1.83 ± 0.13	114.4	7.01	5.29 ± 0.09
		7.12	5.80 ± 0.10		7.54	4.41 ± 0.07
a	116.7	7.11	5.80 ± 0.10	116.6	7.11	4.91 ± 0.08
		7.73	4.94 ± 0.05		7.76	5.14 ± 0.07

[a] In DMSO-d_6 at 30°C. ^1H chemical shifts are relative to internal TSP, while ^{15}N chemical shifts were determined relative to external CH_3NO_2 but are reported relative to $NH_3(l)$.

[b] Ref. 44.

2). The effects of epimerization on the bond lengths and bond angles in the B ring are highlighted in structures **7** and **8** in which the significant differences in bond length (**7**) and bond angle (**8**) between CNCbl and CN-8-epiCbl are given for the B ring and its peripheral attachments. The uncertainties connected with the bond lengths and angles at C42 are due to its half-site occupancy in two different positions. The substantial differences in geometry about the amides must be attributed, at least in part, to differences in hydrogen bonding to these functionalities in the two structures. Thus, in CNCbl, the *d* amide carbonyl is hydrogen bonded to N28 of a symmetry related molecule (3.24 Å) while in CN-8-epiCbl, it is hydrogen bonded to two waters of crystallization (W12 at 2.88 Å and W15 at 2.65 Å), and the *d* amide nitrogen is hydrogen bonded to W6 (2.99 Å). Similarly, the *c* amide nitrogen in CNCbl is hydrogen bonded to O5 (3.00 Å) of a symmetry related molecule and a water of crystallization (2.69 Å) and the *c* carbonyl is hydrogen bonded to another water of crystallization (2.64 Å), while in CN-8-epiCbl, the *c* amide nitrogen is hydrogen bonded to the *b* amide carbonyl O33 (2.83 Å) of a symmetry related molecule, and the *c* amide carbonyl oxygen is hydrogen bonded to a water (W10, 2.69 Å), and to the *b* amide nitrogen (N34, 2.98 Å) of a symmetry related molecule.

In addition to the local effects of C8 epimerization on the B ring conformation, more global conformational effects on the corrin ring are evident in Fig. 9 and in the corrin carbon torsion angles, bond lengths and bond angles listed in Table 2. Significant bond length and bond angle differences occur virtually throughout the corrin, with the exception of the A ring (Table 2). Glusker has characterized the gross conformations of the corrin ring by use of the corrin fold angle along the Co···C10 axis, defined as the angle between the least-squares plane including N21, C4, C5, C6, N22, C9, and C10, and that including N24, C16, C15, C14, N23, C11, and C10. For CN-8-epiCbl, the former plane has a mean deviation of 0.07 Å, the latter a mean deviation of 0.02 Å, and the angle between these planes is 23.8°. This is a substantially more severe corrin fold than in CNCbl (17.7°) and, in fact, is the largest corrin fold angle known.[61] This increased upward folding is accomplished mostly by an upward displacement of the former plane (i.e., the "north" half of the corrin) as there is relatively little displacement of the corrin atoms from C13 to C18 (Fig. 9). This phenomenon is reflected in the torsion angles among the corrin ring carbons as seen in Table 2. Those torsion angles including carbons C19—C1, etc., through C15 are, in general, significantly different in the two structures, while those including C12 through C2 are not. In addition to these global conformational changes, we note that there is a significant change in the pucker of the C ring such that C12 is displaced downward in 8-

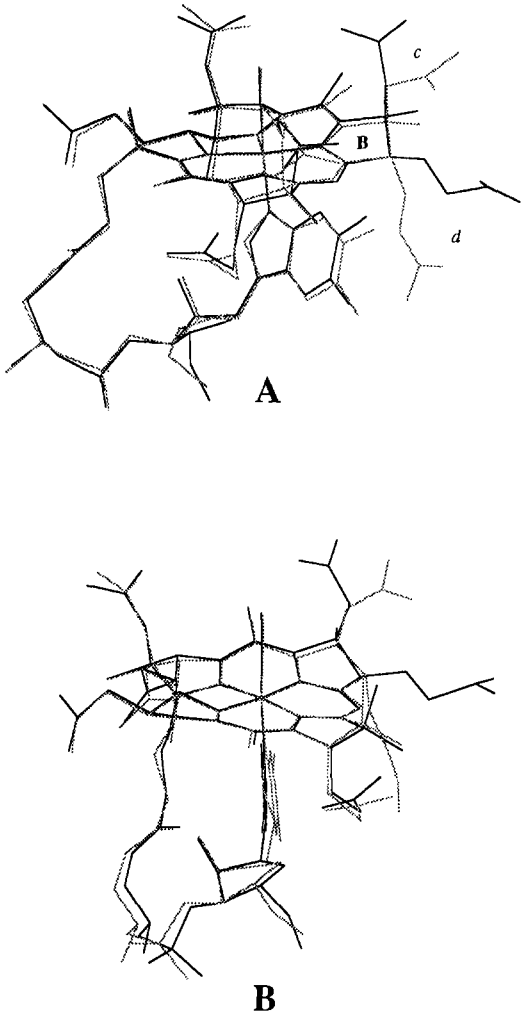

Fig. 9. Structure of CN-8-epiCbl (dark lines) super imposed on CNCbl (light lines), viewed from above the corrin ring along the pyrrole C · · · pyrrole A axis, showing the epimerization at C8 (A), and viewed from above the corrin ring along the C53 · · · C15 axis (B).

epiCbl. This leads to large displacement of the C46 and C47 methyl groups as seen in Fig. 9B and in the torsion angles involving these carbons in Table 2.

It is interesting to compare the structural changes accompanying epimerization of CNCbl at C8 to those accompanying epimerization at C13. In CN-13-epiCbl,[18] there are large differences in the inner sphere geometry, including a 0.17 Å shortening of the Co—C bond and a 0.08 Å lengthening of the axial Co—N bond. The C pyrrole ring, the site of epimerization, is twisted by about 11° such that C13 is displaced upward and C12 is displaced downward, while C11, C14, and N23 have very small displacements. This distortion allows the *c* side chain to adopt an "upwardly" axial position in CN-13-epiCbl in contrast to the equatorial position adopted by the epimerized *d* side chain in CN-8-epiCbl. In addition, the C pyrrole ring distortion in CN-13-epiCbl moves the C46 methyl group from an "upwardly" axial position to an equatorial position and the C47 methyl from an equatorial position to "downwardly" axial position. The corrin ring fold angle in CN-13-epiCbl (21.8°) is again increased from that in CNCbl, but is not as large as that in CN-8-epiCbl. Again, this increased corrin fold is caused primarily by an upward tilt of the "northern" plane as there is little displacement of the C14—C18 carbons.

The NMR spectra of CN-8-epiCbl clearly show the effect of the inversion of configuration at C8, relative to CNCbl. Thus, in CN-8-epiCbl, the C8 proton shows a strong NOE to the axial nucleotide B4 proton, confirming that the C8 proton faces "downward" in this isomer. In addition, no NOE crosspeaks are seen between the C8 proton and the C37 methylene protons is the ROESY spectrum of CN-8-epiCbl although such NOEs have been found for every other Cbl for which data are available. This confirms that the C8 proton and the *c* acetamide side chain are on opposite sides of the corrin ring. Furthermore, NOEs observed between C41H′ and C37H′, and between C41H″ and both of the C37 protons do not occur in normal cobalamins in which the *c* and *d* side chains are on opposite sides of the B ring.

The difference in ^{15}N and ^{1}H chemical shifts of the *d* amide between CNCbl and CN-8-epiCbl also shows the effect of epimerization of this side chain in CN-8-epiCbl. Moreover, the differences in the *c* amide ^{1}H chemical shifts and the low proton chemical shift thermal gradient for the *c* amide *syn* proton strongly suggest that the *c* amide is a proton donor in an intramolecular hydrogen bond in CN-8-epiCbl in solution which is absent in CNCbl. This hydrogen bond is not present in the crystal structure, in which the *c* and *d* amides are involved in various hydrogen bonded interactions with heteroatoms on symmetry related molecules and with waters of crystallization as described above. However, inspection of semi-space filling models of CN-8-epiCbl shows that when the *d* side chain is on the equatorial position on the B pyrrole ring, the *c* and *d* amide groups may be brought into sufficiently close proximity to allow formation of a hydrogen bond involving the *c* amide N—H and the *d* amide carbonyl oxygen.

The complete assignments of the ^{13}C spectrum of CN-8-epiCbl permits a comparison of these ^{13}C chemical shifts with those of CNCbl[22,23] in order to attempt to assess the effect of epimerization on ^{13}C chemical shifts. This comparison is given in Table 3 as the signed difference in chemical shift between

CNCbl and CN-8-epiCbl and the significant differences ($|\Delta\delta| \geq 0.25$ ppm) are highlighted in structure

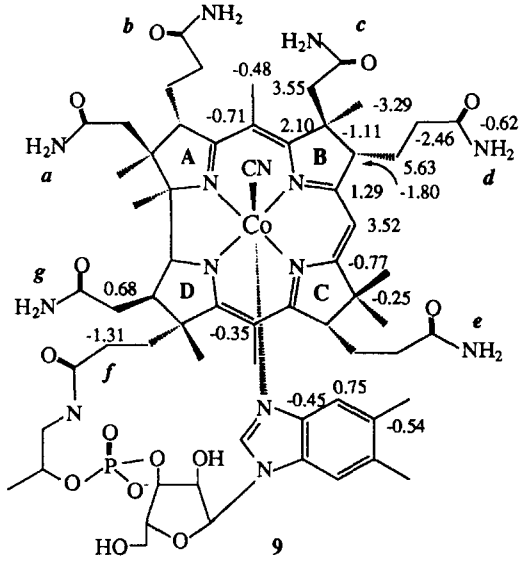

9

9. The corrin B ring peripheral substituents, including the C41, C42, and C37 methylene groups and the C36 methyl group, show large chemical shift differences, as expected. While chemical shift differences of -1.11 to 2.10 ppm occur for the B ring carbon atoms themselves, the largest corrin ring chemical shift difference occurs at C10, and significant differences occur from C4 through C12. These chemical shift differences roughly correspond to the corrin ring conformational differences discussed above and revealed by the corrin carbon torsion angles (Table 2). In addition, there are significant chemical shift differences at the axial nucleotide carbons B4, B5, and B9, at the *f* side chain methylene group, C56, and inexplicably, at C60. The chemical shift differences at the axial nucleotide carbons could reflect the slight tilt of the Bzm in CN-8-epiCbl, or a chemical shift effect of the proximity of the *d* side chain to the upper part of the axial nucleotide in CNCbl which is removed in the C8 epimer since the *d* side chain is equatorial. However, these chemical shifts could also be affected by a difference in the strength of coordination of the axial benzimidazole ligand to the metal atom in CN-8-epiCbl and CNCbl, since the axial benzimidazole ^{13}C chemical shifts of base-on RCbls are well known to be sensitive to the strength of donation from the B3 nitrogen to the cobalt atom.[62,63] Such differential axial ligand coordination could also be the cause of the chemical shift difference at C56 since the nucleotide loop is known to be strained in base-on RCbls and the amount of strain is sensitive to the strength of benzimidazole coordination.[64] Comparison of the chemical shift of C56 in CNCbl and in $(CN)_2$Cbl[22,23] shows that this carbon does, indeed, show the effects of this strain.

In summary, the synthesis of the putative CN-8-epiCbl through borohydride reduction of CNCbl-*c*-lactone has been reexamined. Reaction conditions have been modified to increase greatly the yield of this analogue. In addition, this derivative has been unambiguously shown to be the C8 epimer of CNCbl by FAB MS, X-ray crystallography, and ^1H, ^{13}C, and ^{15}N NMR, which also allow a comparison of the crystal and solution structures of the analogue. This improved synthesis has now provided CN-8-epiCbl in ample quantities for studies to assess the importance of the *d* amide side chain in Co—C bond thermal homolysis as well as its role in the association of Cbls with B_{12}-binding proteins and enzymes. Such studies are currently in progress.

Acknowledgements—This research was supported by the National Institute of General Medical Sciences through grant GM 48858, the National Science Foundation EPSCoR program through grant EHR 9108767, the State of Mississippi, and Mississippi State University. The authors are grateful to Dr. Clemens Anklin, Bruker Instruments, Inc., Billerica, MA, for providing the 600 MHz NMR spectra of CN-8-epiCbl, and to Dr. Rickey P. Hicks and Dr. John Young of this department for assistance with NMR experiments at other field strengths. J.D.Z. and E.J.V. wish to thank the Office of Naval Research for support of X-ray crystallography.

Supplementary material—The atomic coordinates have been deposited with the Cambridge Crystallographic Data Centre. Tables of the atomic coordinations of CN-8-epiCbl, tentative ^{13}C NMR assignments of CNCbl-*c*-lactone and CN-8-epiCbl-*c*-COO^-, anisotropic thermal parameters for all non-hydrogen atoms, bond distances and bond angles between all non-hydrogen atoms and their estimated, calculated coordinates of all hydrogen atoms, intermolecular contacts, NMR connectivities for CN-8-epiCbl in D_2O, NOESY connectivities for CN-8-epiCbl in DMSO-d_6, a unit cell packing diagram, and an ORTEP diagram of CN-8-epiCbl (26 pages) are available from the authors.

REFERENCES

1. Abbreviations: Cbl, cobalamin; AdoCbl, 5′-deoxyadenosylcobalamin (coenzyme B_{12}); CN-13-epiCbl, cyano-13-epicobalamin; Ado-13-epiCbl, 5′-deoxyadenosyl-13-epicobalamin (neocoenzyme B_{12}); CN-8-epiCbl, cyano-8-epicobalamin; CN-8-epiCbl-*c*-COO^-, cyano-8-epicobalamin-*c*-monocarboxylate [Coα-(α-5,6-dimethylbenzimidazolyl)-Coβ-cyano-8-epicobamic acid *a,b,d,e,g*-pentaamide]; CNCbl-*c*-lactone, cyanocobalamin-*c*-lactone; ECDI,

1-ethyl-3-(3-dimethylamino)propylcarbodiimide; 10-Cl-CNCbl-*c*-lactone, 10-chlorocyanocobalamin-*c*-lactone; TSP, (trimethylsilyl)propionate.

In the NMR assignments, prime and double prime notations denote the downfield and upfield signals, respectively, of diastereotopic methylene protons, or the downfield (*anti*) and upfield (*syn*) protons, respectively, of a pair of primary amide protons.

2. T. Toraya, T. Shirakashi, S. Fukui and H. P. C. Hogenkamp, *Biochemistry* 1975, **14**, 3949.
3. T. Toraya, E. Krodel, A. S. Mildvan and R. H. Abeles, *Biochemistry* 1979, **18**, 417.
4. C. G. D. Morley, R. L. Blakley and H. P. C. Hogenkamp, *Biochemistry* 1968, **7**, 1231.
5. M. I. Yakusheva, A. A. Poznanskaya, T. A. Pospelova, I. P. Rudakova, A. M. Yurkevich and V. A. Yakovlev, *Biochim. Biophys. Acta* 1977, **484**, 216.
6. E. L. Lien, L. Ellenbogen, P. Y. Law and J. M. Wood, *J. Biol. Chem.* 1974, **249**, 890.
7. J. B. Armitage, J. R. Cannon, A. W. Johnson, L. F. J. Parker, E. L. Smith, W. H. Stafford and A. R. Todd, *J. Chem. Soc.* 1953, 3349.
8. K. Bernhauer, F. Wagner, H. Beisbarth, P. Rietz and H. Vogelmann, *Biochem. Z.* 1966, **344**, 289.
9. H. M. Marques, D. C. Scooby, M. Victor and K. L. Brown, *Inorg. Chim. Acta* 1989, **162**, 151.
10. R. Bonnett, J. R. Cannon, U. M. Clark, A. W. Johnson, L. F. J. Parker, E. L. Smith and A. Todd, *J. Chem. Soc.* 1957, 1158.
11. R. Bonnett, J. M. Godfrey, V. B. Math, E. Edmond, H. Evans and O. J. R. Hodder, *Nature* 1971, **229**, 473.
12. R. Bonnett, J. M. Godfrey and V. B. Math, *J. Chem. Soc. C.* 1971, 3736.
13. A. R. Fersht, J. P. Shi, J. Knill-Jones, D. M. Lowe, A. J. Wilkinson, D. M. Blow, P. Brick, M. M. Y. Waye and G. Winter, *Nature* 1985, **314**, 235.
14. K. L. Brown and H. B. Brooks, *Inorg. Chem.* 1991, **30**, 3420.
15. R. G. Finke and B. P. Hay, *Inorg. Chem.* 1984, **23**, 3041.
16. B. P. Hay and R. G. Finke, *J. Am. Chem. Soc.* 1986, **108**, 4820.
17. K. L. Brown, H. B. Brooks, D. Behnke and D. W. Jacobsen, *J. Biol. Chem.* 1991, **266**, 6737.
18. H. Stoeckli-Evans, E. Edmond and D. C. Hodgkin, *J. Chem. Soc. Perkin Trans. II* 1972, 602.
19. P. Rapp and U. Oltersdorf, *Hoppe-Seyler's Z. Physiol. Chem.* 1973, **354**, 32.
20. D. W. Jacobsen, R. Green and K. L. Brown, *Methods Enzymol.* 1986, **123**, 14.
21. K. L. Brown, X. Zou and L. Salmon, *Inorg. Chem.* 1991, **30**, 1949.
22. T. G. Pagano and L. G. Marzilli, *Biochemistry* 1989, **28**, 7213.
23. K. L. Brown, H. B. Brooks, B. D. Gupta, M. Victor, H. M. Marques, D. C. Scooby, W. J. Goux and R. Timkovich, *Inorg. Chem.* 1991, **30**, 3430.
24. L. Braunschweiler and R. R. Ernst, *J. Magn. Reson.* 1983, **53**, 521.
25. D. G. Davis and A. Bax, *J. Am. Chem. Soc.* 1985, **107**, 2820.
26. A. Bax and D. G. Davis, *J. Magn. Reson.* 1985, **65**, 355.
27. A. A. Bothner-By, R. L. Stephens, J. Lee, C. D. Warren and R. W. Jeanloz, *J. Am. Chem. Soc.* 1984, **106**, 811.
28. A. Bax and D. G. Davis, *J. Magn. Reson.* 1985, **63**, 207.
29. A. Bax, R. G. Griffey and B. L. Hawkins, *J. Am. Chem. Soc.* 1983, **105**, 7188.
30. M. R. Bendell, D. T. Pegg and D. M. Doddrell, *J. Magn. Reson.* 1983, **52**, 81.
31. A. Bax and S. Subramanian, *J. Magn. Reson.* 1986, **67**, 565.
32. M. F. Summers, L. G. Marzilli and A. Bax, *J. Am. Chem. Soc.* 1986, **108**, 4285.
33. A. Bax and M. F. Summers, *J. Am. Chem. Soc.* 1986, **108**, 2093.
34. P. R. Srinivasen and R. L. Lichter, *J. Magn. Reson.* 1977, **28**, 227.
35. G. M. Sheldrick, *Acta Cryst.* 1990, **A46**, 467.
36. G. M. Sheldrick, 1995, in preparation.
37. H. D. Flack, *Acta Cryst.* 1983, **A39**, 876.
38. F. Wagner, *Proc. R. Soc. London* 1965, **A288**, 344.
39. C. Brink-Shoemaker, D. W. J. Craikshonk, D. C. Hodgkin, M. K. Kanper and D. Pilling, *Proc. R. Soc. London* 1964, **A228**, 1.
40. K. L. Brown and X. Zou, *J. Am. Chem. Soc.* 1992, **114**, 9643.
41. J. Jeener, B. H. Meier, P. Bachmann and R. R. Ernst, *J. Chem. Phys.* 1979, **71**, 4546.
42. S. Macura and R. R. Ernst, *Mol. Phys.* 1980, **41**, 1980.
43. A. Bax, L. G. Marzilli and M. F. Summers, *J. Am. Chem. Soc.* 1987, **109**, 566.
44. T. G. Pagano, P. G. Yohannes, B. P. Hay, J. R. Scott, R. G. Finke and L. G. Marzilli, *J. Am. Chem. Soc.* 1989, **111**, 1484.
45. T. G. Pagano, L. G. Marzilli, M. M. Flocco, C. Tasi, H. L. Carrell and J. P. Glusker, *J. Am. Chem. Soc.* 1991, **113**, 531.
46. Y. W. Alelyunas, P. E. Fleming, R. G. Finke, T. G. Pagano and L. G. Marzilli, *J. Am. Chem. Soc.* 1991, **113**, 3781.
47. K. L. Brown and D. R. Evans, *Inorg. Chem.* 1993, **32**, 2544.
48. P. E. Hansen, *Prog. Nucl. Magn. Reson. Spectrosc.* 1981, **14**, 175.
49. K. L. Brown, X. Zou, S. R. Savon and D. W. Jacobsen, *Biochemistry* 1993, **32**, 8421.
50. T. J. DiFeo, R. A. Schiksnis, R. K. Kohli, S. I. Opella and A. Nath, *Magn. Reson. Chem.* 1989, **27**, 127.
51. K. L. Brown, H. B. Brooks, X. Zou, M. Victor, A. Ray and R. Timkovich, *Inorg. Chem.* 1990, **29**, 4841.
52. K. L. Brown and X. Zou, *J. Am. Chem. Soc.* 1993, **115**, 1478.
53. L. H. Piette, J. D. Ray and R. A. Ogg, *J. Mol. Spectrosc.* 1958, **2**, 66.
54. D. E. Dorman and F. A. Bovay, *J. Org. Chem.* 1973, **38**, 1719.

55. A. DeMarco and M. Linas, *Org. Magn. Reson.* 1979, **12**, 454.
56. A. G. Redfield and S. Waelder, *J. Am. Chem. Soc.* 1979, **101**, 6151.
57. C. L. Perrin, E. R. Johnston, C. P. Lollo and P. A. Kobrin, *J. Am. Chem. Soc.* 1981, **103**, 4691.
58. H. Kessler, *Angew. Chem., Int. Ed. Engl.* 1982, **21**, 512.
59. Y. A. Ovchinnokov and V. T. Ivanov, *Tetrahedron* 1974, **30**, 1871.
60. V. B. Pett, M. N. Liebmon, P. Murray-Rust, K. Prasad and J. P. Glusker, *J. Am. Chem. Soc.* 1987, **109**, 3207.
61. J. P. Glusker, in "B_{12}" (Edited by D. Dolphin), pp. 23–106. Wiley, New York (1982).
62. K. L. Brown and J. M. Hakimi, *J. Am. Chem. Soc.* 1986, **108**, 496.
63. K. L. Brown and G.-Z. Wu, *Inorg Chem.* 1994, **33**, 4122.
64. K. L. Brown and J. M. Hakimi and D. W. Jacobsen, *J. Am. Chem. Soc.* 1984, **106**, 7894.